Excitation-density-dependent generation of broadband terahertz radiation in an asymmetrically excited photoconductive antenna

Prashanth C. Upadhya,[1,*] Wenhui Fan,[1] Andrew Burnett,[1] John Cunningham,[1] A. Giles Davies,[1] Edmund H. Linfield,[1] James Lloyd-Hughes,[2] Enrique Castro-Camus,[2] Michael B. Johnston,[2] and Harvey Beere[3]

[1]*School of Electronic and Electrical Engineering, University of Leeds, Leeds LS2 9JT, UK*
[2]*Clarendon Laboratory, University of Oxford, Parks Road, Oxford OX1 3PU, UK*
[3]*Cavendish Laboratory, University of Cambridge, Cambridge CB3 0HE, UK*
[*]*Corresponding author: p.upadhya@leeds.ac.uk*

Received February 8, 2007; revised May 25, 2007; accepted June 22, 2007;
posted June 26, 2007 (Doc. ID 79951); published August 2, 2007

The generation of terahertz (THz) transients in photoconductive emitters has been studied by varying the spatial extent and density of the optically excited photocarriers in asymmetrically excited, biased low-temperature-grown GaAs antenna structures. We find a pronounced dependence of the THz pulse intensity and broadband (>6.0 THz) spectral distribution on the pump excitation density and simulate this with a three-dimensional carrier dynamics model. We attribute the observed variation in THz emission to changes in the strength of the screening field. © 2007 Optical Society of America

OCIS codes: 260.3090, 320.7120.

Generating electromagnetic pulses using photoconductive semiconductor structures has, during the past few years, evolved into a comprehensive technique for exploring the terahertz (THz) frequency range [1–4]. This technique is based on the impulsive excitation of a biased antenna by ultrashort (<150 fs) optical pulses, with the resulting charge carrier ensemble producing a transient photocurrent or, equivalently, a time-dependent dipole moment across the gap between electrodes. This radiates a subpicosecond pulse with temporal coherence into free space, with a spectral content that depends on the charge carrier dynamics governing the time evolution of the current transient under the bias field.

The time-varying transient photocurrent in an antenna is given by $\partial J/\partial t = en\partial v/\partial t + ev\partial n/\partial t$, where e is the carrier charge, n is the carrier density, and v is the carrier velocity [5]. Therefore, the emitted THz radiation depends strongly on both the photoinduced carrier density ($\partial J/\partial t \propto \partial n/\partial t \propto$ pump fluence) and the local electric field across the photoconductive gap, which produces an acceleration of mobile charges ($\partial J/\partial t \propto \partial v/\partial t$). High optical fluence as well as high electric field strength are thus central to the efficient production of THz radiation. However, owing to device-related properties, the THz electric field produced by an antenna eventually saturates as either the applied optical fluence or voltage is increased [6], and this often limits the utilization of the maximum power available from the pump laser.

The emission characteristics of a photoconductive antenna can also be influenced by the antenna design [7,8]. Studies have shown that high-power THz pulses with a broad spectral distribution can be generated using large aperture, planar strip-line photoconductive antennas that allow the utilization of high optical energies and high bias fields [2,3,6]. For planar strip-line structures, the emission efficiency can be further enhanced by nonuniform optical illumination of the photoconductive gap, across which an asymmetric distribution of carriers is being excited [2,4,9–12]. Illuminating the gap close to the anode electrode (asymmetric excitation of the switch gap) produces a relative enhancement in the THz field and a shorter THz pulse, i.e., a broader frequency distribution. This has been attributed to the higher effective mobility of the induced electron population near the anode, compared with the mobility of the hole population at the cathode, which leads to greater carrier acceleration at the anode [2,9,10].

In this Letter, we present a systematic investigation of the dependence of the spectral composition and power of THz pulses generated from an asymmetrically excited, biased photoconductive antenna, on the density of excited carriers. We show how the focus of the near-infrared incident radiation onto the photoconductive gap, and hence the density of excited carriers, can be optimized to maximize the spectral bandwidth (>6.0 THz) and THz power generated. We also use a three-dimensional Monte Carlo carrier dynamics model to simulate the emission characteristics at different excitation densities, for comparison with experimental data.

Our emitter comprised two thermally evaporated NiCr/Au electrodes separated by a 0.4 mm gap, formed on an LT-GaAs surface [see inset of Fig. 1(b)]. The 1 μm thick LT-GaAs layer was grown on a 1.0 mm thick undoped GaAs substrate and had a short photocarrier lifetime (~3.8 ps). A bias field of 2.5 kV/cm, modulated at 10 kHz, was applied across the emitter. A 10 fs Ti:sapphire laser of 175 mW average power was focused on the edge of one of the two NiCr/Au electrodes of the LT-GaAs emitter to generate THz pulses. The emitted radiation was collected in the "reflection" direction from the photoconductive emitter (i.e., in the direction of the reflected pump la-

ser beam), thereby avoiding dispersion–absorption of the THz radiation in the GaAs substrate [4]. The spatial distribution of the electric field under the external bias is highly nonuniform, with 80% of the field expected to be concentrated within an ~ 20 μm region close to the anode. By focusing the laser near the anode, we obtained a high photocarrier density ($>10^{18}$ cm^{-3}) in this high-field (>30 kV/cm) region [10]. The optical excitation density was varied by changing the focus, i.e., the spot size, of the pump laser on the emitter while keeping the average laser power constant. In this way, both the photoinduced carrier density and the dynamics of electric field screening were varied [13], and hence the THz emission was altered. The diameter of the Gaussian beam waist on the emitter surface at 90% of its intensity spread was defined to be the size of the excitation area. The generated THz radiation was characterized by electro-optic sampling, by focusing the THz beam onto a 150 μm thick ⟨110⟩ orientated undoped GaP detector with nearly diffraction-limited spot size.

Figure 1(a) shows the dependence of the generated THz pulse on the near-infrared laser spot size for a fixed average power (175 mW) with the laser spot focused on the edge of the anode. Experimentally, the laser was focused so that a part of the spot overlapped the anode and the spot position was then optimized to obtain the maximum THz amplitude. A decreasing spot size results both in a substantial increase in the THz pulse amplitude and also in a shortening of the pulse width [to a full width at half-maxima (FWHM) <110 fs], with the pulse peak shifting to earlier times. These features indicate a larger rate of change of photoinduced current density with decreasing spot size. Commensurately, in the frequency domain [Fig. 1(b)], as the excitation spot size is reduced, the amplitude of the THz spectra increases progressively, and the position of the THz peak shifts to higher frequencies.

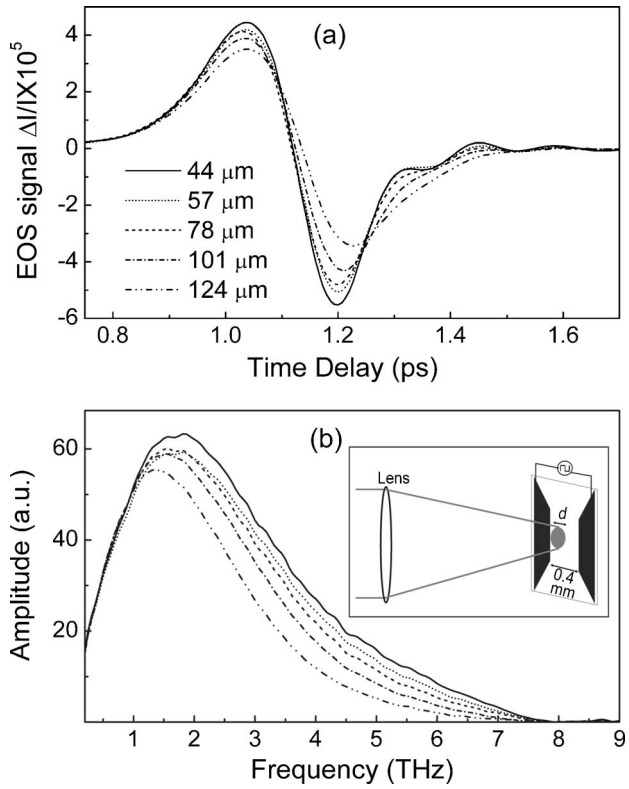

Fig. 1. (a) Temporal THz waveforms measured with a 150 μm thick ⟨110⟩ GaP electro-optic sensor for different laser spot sizes. Note that at smaller spot sizes, pronounced phonon oscillations are seen after the initial transients. (b) Fourier-transform amplitude spectra of the data shown in (a). Inset: schematic geometry of the electrodes used in the LT-GaAs photoconductive emitter. The circular spot indicates the position of the asymmetric laser excitation.

Figure 2 shows that there is a rapid change in the spectral position of the THz peak for spot sizes >80 μm and that the integrated power ($\propto$ energy content) of the THz pulse displays an almost linear reduction as the spot size is increased, decreasing by 30% when the spot size changes from 44 μm (fluence $\cong 153$ μJ/cm^2 at 175 mW) to 124 μm (fluence $\cong 19$ μJ/cm^2 at 175 mW). We note that the THz electric field amplitude begins to exhibit pump-fluence-dependent saturation behavior if the incident laser power is increased beyond 200 mW, and spectral power does not increase significantly for smaller spot sizes.

To further understand the physical mechanism behind the THz generation and its dependence on excitation density, a semiclassical Monte Carlo model was used to simulate THz emission from a photoconductive antenna at various excitation densities. The simulation was based on a three-dimensional carrier dynamics model for an LT-GaAs photoconductive antenna, the details of which can be found elsewhere [9,14]. The model incorporates the effect of the carrier lifetime in LT-GaAs on the time evolution of the photocurrent transients in the antenna, with the carrier lifetime being predominantly determined by the carrier capture in midgap states, created by the defects originating from arsenic clusters. An exponential reduction in the number of photoexcited carriers was used to model carrier capture by defects in LT-GaAs [15] (for which, a lifetime of 3.8 ps was used, as determined from transient reflectance measure-

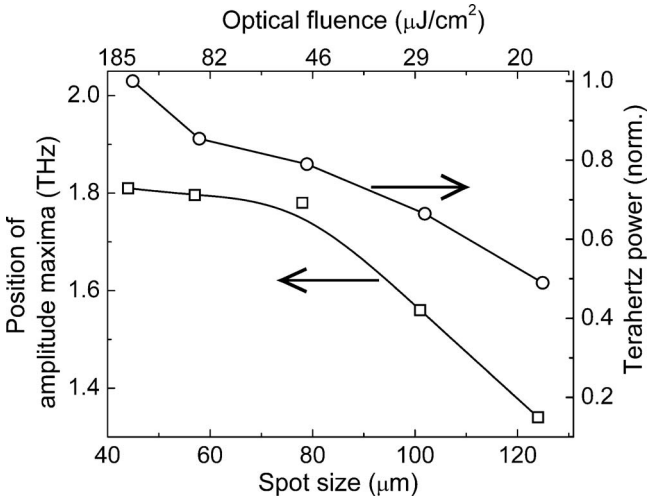

Fig. 2. Position of the THz amplitude maxima (left axis) and integrated spectral THz pulse power (right axis) as a function of spot size. The upper axis gives the corresponding optical fluence of the laser pulse.

ments). A pump pulse duration of 10 fs was assumed, and the pump spot size was taken to have a Gaussian spatial distribution, centered near the edge of the anode. The simulated spot sizes were chosen to give similar percentage coverage of the gap as in the experiment (e.g., a $\sigma=11\%$ spot size in simulation thus corresponds to $d=44$ μm in the experiment, where σ is the standard deviation of the Gaussian distribution).

The duration of the simulated THz electric field pulse shortens as the pump spot size is reduced, producing greater power at high frequencies, as found experimentally. In the frequency domain, the FWHM of the spectra of the simulated electric field agrees well with the experimental data [Fig. 3], except for the smallest spot size. We attribute this discrepancy to an approximation used in the model that the potential distribution changes slowly (Brooks–Herring approximation), which no longer holds at high photoinduced carrier density (i.e., short Debye length) [14]. Note that the mean momentum scattering rate of the Γ-valley electrons at zero simulation time (peak of pump pulse intensity), summed over all scattering mechanisms [15], shows no significant dependence on spot size.

Our results can be explained by the dipole polarization field, $P=nqx$ (where n is the density of dipoles, q is the electron charge, and qx is the dipole moment) increasing with photoexcited carrier density, i.e., a smaller spot size produces a stronger screening field (for a given dipole moment). Thus, the applied electric field becomes screened on shorter time scales [16] as the spot size is reduced [inset of Fig. 3]. Carrier momentum scattering (which produces the rapid decay in the THz electric field) then occurs at earlier times, resulting in shorter emitted pulse durations, as observed experimentally.

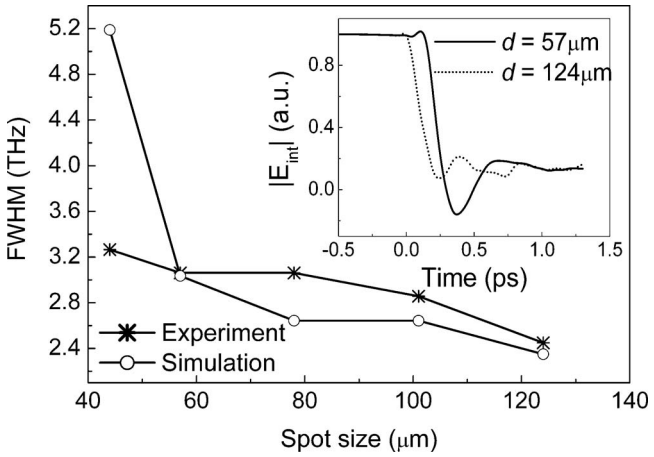

Fig. 3. Comparison of the FWHM of the simulated THz emission with the experiment, as a function of spot size. Inset: time dependence of the screening inside a photoconductive switch for two pump spot sizes. E_{int} is the internal electric field at a position in the gap equivalent to the center of the laser spot, and the time it takes to reach a constant low value is a good indication of the time taken for photocarriers to screen the applied electric field. This screening time decreases from ~0.35 ps for $d=124$ μm to ~0.2 ps at $d=57$ μm. The screened electric field recovers at times greater than 0.4 ps because of the trapping of photoexcited carriers (a carrier lifetime of 3.8 ps was used in the simulation).

In summary, we have investigated the dynamics of THz emission in asymmetrically excited photoconductive emitters as the near-infrared spot size is changed. For smaller spot sizes, the increased excitation density enhances the emitted THz power as well as broadening the frequency bandwidth. Simulations show that a smaller spot size produces a stronger, faster screening of the applied field, resulting in shorter THz transients. These results will be invaluable for designing and optimizing photoconductive emitters across a number of applications, including spectroscopy and imaging, where greater THz power, covering a broader frequency range, is highly desirable.

This work was supported by the Research Councils UK (Basic Technology Programme), EPSRC (UK), The Royal Society (UK), CONACyT (Mexico), DSTL, and the European Commission [TeraNova, an IST FP6 Integrated project (IST-511415)].

References

1. J. T. Darrow, B. B. Hu, X.-C. Zhang, and D. H. Auston, Opt. Lett. **15**, 323 (1990).
2. N. Katzenellenbogen and D. Grischkowsky, Appl. Phys. Lett. **58**, 222 (1991).
3. P. Uhd Jepsen, R. H. Jacobsen, and S. R. Keiding, J. Opt. Soc. Am. B **13**, 2424 (1996).
4. Y. C. Shen, P. C. Upadhya, E. H. Linfield, H. E. Beere, and A. G. Davies, Appl. Phys. Lett. **83**, 3117 (2003).
5. Z. Piao, M. Tani, and K. Sakai, Jpn. J. Appl. Phys., Part 1 **39**, 96 (2000).
6. J. T. Darrow, X.-C. Zhang, D. H. Auston, and J. D. Morse, IEEE J. Quantum Electron. **28**, 1607 (1992).
7. M. Tani, S. Matsuura, K. Sakai, and S. Nakashima, Appl. Opt. **36**, 7853 (1997).
8. Y. Cai, I. Brener, J. Lopata, J. Wynn, L. Pfeiffer, and J. Federici, Appl. Phys. Lett. **71**, 2076 (1997).
9. E. Castro-Camus, J. Lloyd-Hughes, and M. B. Johnston, Phys. Rev. B **71**, 195301 (2005).
10. Y. C. Shen, P. C. Upadhya, E. H. Linfield, H. E. Beere, and A. G. Davies, Phys. Rev. B **69**, 235325 (2004).
11. E. Sano and T. Shibata, Appl. Phys. Lett. **55**, 2748 (1989).
12. U. D. Keil and D. R. Dykaar, IEEE J. Quantum Electron. **32**, 1664 (1996).
13. D. S. Kim and D. S. Citrin, Appl. Phys. Lett. **88**, 161117 (2006).
14. M. B. Johnston, D. M. Whittaker, A. Corchia, A. G. Davies, and E. H. Linfield, Phys. Rev. B **65**, 165301 (2002).
15. J. Lloyd-Hughes, E. Castro-Camus, M. D. Fraser, C. Jagadish, and M. B. Johnston, Phys. Rev. B **70**, 235330 (2004).
16. J. E. Pedersen, V. G. Lyssenko, J. M. Hvam, P. Uhd Jepsen, S. R. Keiding, C. B. Sørensen, and P. E. Lindelof, Appl. Phys. Lett. **62**, 1265 (1993).